A 160-Femtosecond Optical Image Processor Based on a Conjugated Polymer

Craig Halvorson, Andrew Hays, Brett Kraabel, Rulian Wu, Fred Wudl, Alan J. Heeger

Degenerate ground-state conjugated polymers exhibit large third-order nonlinear optical susceptibilities, including substantial two-photon absorption. With the use of a machine architecture suited to these material properties, ultrafast optical processors are possible. A four-wave mixing optical correlator was built with an air-stable, processable, degenerate ground-state conjugated polymer, poly(1,6-heptadiester). The continuously updatable processor correlates two 5000-pixel images in less than 160 femtoseconds, achieving peak processing rates of 3×10^{16} operations per second.

Conjugated polymers exhibit large third-order nonlinear optical (NLO) susceptibilities; resonant and nonresonant third-order NLO susceptibilities with magnitudes of 10^{-7} and 10^{-8} electrostatic units, respectively, have been measured in the simplest conjugated polymer, *trans*-polyacetylene (*1*, *2*). Because third-order effects allow light beams to interact with other light beams within the nonlinear medium and because the nonresonant response occurs at subfemtosecond times, all-optical computers that operate on a femtosecond time scale should be possible.

For third-order NLO devices that involve waveguiding, the figure of merit is the nonlinear refractive index divided by the sum of linear and nonlinear absorptions (*3*). Near resonance, one would expect the nonlinear refractive index susceptibility, $\mathrm{Re}\chi^{(3)}(\omega;\omega,-\omega,\omega)$ (the real component of the susceptibility χ), to be comparable in magnitude to the two-photon absorption susceptibility, $\mathrm{Im}\chi^{(3)}(\omega;\omega,-\omega,\omega)$ (the imaginary component of χ). Measurements of these two quantities for oriented *trans*-polyacetylene confirm this analysis (*1*, *2*, *4*). If $\mathrm{Re}\chi^{(3)}(\omega;\omega,-\omega,\omega) \approx \mathrm{Im}\chi^{(3)}(\omega;\omega,-\omega,\omega)$, then all-optical waveguiding devices will exhibit poor performance for a very simple reason: They will not be transparent at the intensities needed to operate the device. Therefore, a new approach to third-order NLO devices is required, one that matches to the NLO properties of these materials (*4*).

Four-wave mixing devices use a short optical pathlength in the active medium and are therefore insensitive to two-photon absorption. Such devices have other advantages as well, including the inherent massive parallelism imparted by the spatial modulation of a light beam and the implementation of complex operations—such as correlation (*5*), associative memory (*6*), neural networks (*7*), or matrix multiplication (*8*)—in a single step. The processing operation is implemented directly by the physics of the NLO interaction rather than through complex and slow software programs.

The origin of the large third-order nonlinear response of *trans*-polyacetylene is the degenerate ground state of the conjugated backbone (*9*). The two-fold degenerate ground state was retained in poly(1,6-heptadiester) (PHDE) (*10*).

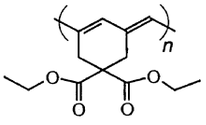

Side groups were added to ensure processability. Because the side groups are electronically isolated from the main chain by σ bonds, they do not seriously affect the optical properties. The resulting material is air-stable and soluble in chloroform, tetrahydrofuran, and other common solvents, allowing spin-casting. The resonant and nonresonant susceptibilities (*11*) of (nonoriented) PHDE are $\chi^{(3)} \approx 5 \times 10^{-10}$ and 6×10^{-11} esu, respectively. The tradeoff versus *trans*-polyacetylene is therefore about one order of magnitude in $\chi^{(3)}$ in return for processability and stability. For our experiments, PHDE was spin cast, in air, from chloroform, resulting in uniform thin films with optical density in the desirable range from 0.5 to 1.0.

A diagram of the matched-filter image correlator is shown in Fig. 1. The pump beam was expanded to a diameter of 25 mm and then split into an object beam (ob), a reference beam (ref), and a read beam (re) of equal pathlength. The object beam and read beam were intensity modulated by optically addressed spatial light modulators (SLMs) and then Fourier-transformed by lenses focused onto the NLO polymer film; the reference beam was reduced to 2 mm in diameter and collimated. The reference and read beams counterpropagated, creating a phase-matching condition that constrained the phase conjugate beam (pc) to emerge counterpropagating to the object beam; the phase conjugate beam was then picked off by a beam splitter. The amplitude of the phase conjugate beam was $A_{pc} \approx A_{ref}A_{re}A^*_{ob}$ (the asterisk denotes the complex conjugate). Because the reference beam was collimated and therefore contained no spatial information, the amplitude of the phase conjugate beam was proportional to $A_{re}A^*_{ob}$. This was equivalent to the cross-correlation of the two-dimensional images placed onto the read and object beams by the SLMs. The phase conjugate beam was then inverse Fourier transformed by a lens and imaged by a charge-coupled device (CCD) array. A spatial filter was used to remove the central maximum from the correlation (*4*).

The pump laser for the correlator was an argon-ion pumped colliding pulse mode-locked laser operating at 620 nm, amplified by a doubled Nd:yttrium-lanthanide-fluorine (YLF) pumped bow-tie amplifier; pulse widths at the PHDE sample were 90 fs, and typical pulse energies were 5 μJ.

The simplest conceptual model of a computer, the Turing machine, includes the ability to process changing data using programmable rules; an optical computer must have this capability. Two nematic liquid-crystal SLMs were used in the correlator, one to enter data (the array of images to be processed) and the other to enter rules (the probe image). The optically addressed SLMs (Micro-Optics P2010) were capable of being updated at video rates (30 Hz).

Figure 2 shows the experimental results for optical correlation between two images (Fig. 2, A and B). The resulting correlation is shown in Fig. 2C. The large peak in Fig. 2C is the correlation intensity between two

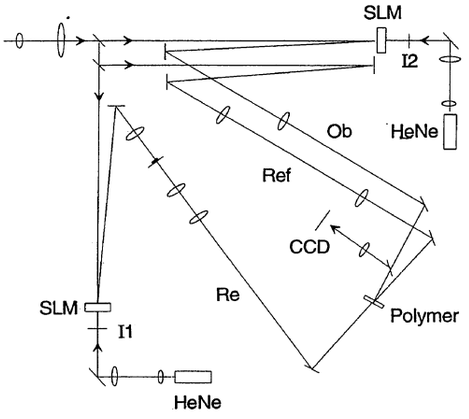

Fig. 1. Schematic diagram of the optical image correlator. Object beam, Ob; reference beam, Ref; read beam, Re; spatial light modulator, SLM; charge-coupled device, CCD; and the images to be correlated, I1 and I2.

Institute for Polymers and Organic Solids, University of California, Santa Barbara, CA 93016, USA.

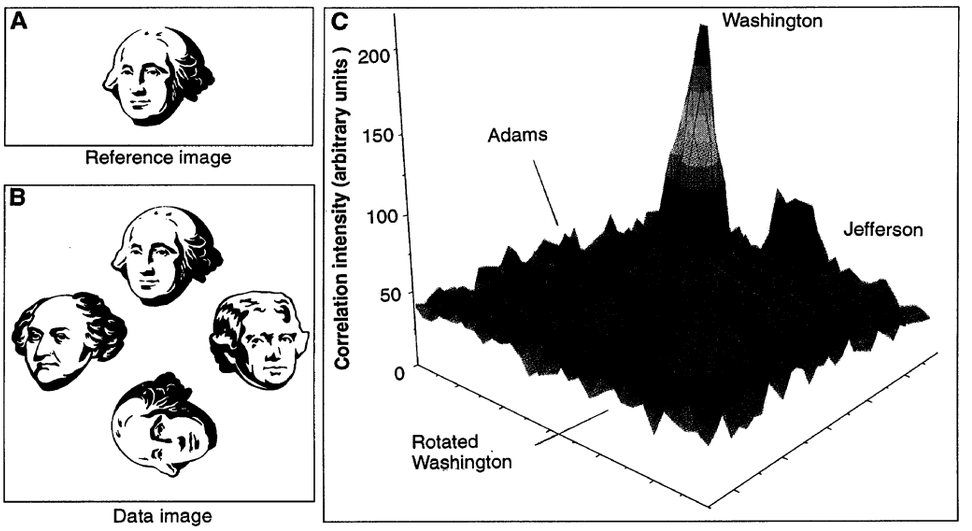

Fig. 2. (**A**) Image of Washington. (**B**) Images of Washington (top), Jefferson (right), Adams (left), and Washington rotated by 90° (bottom). (**C**) Correlation of the images in (A) and (B). The large peak is the correlation intensity between the two images of Washington; the next largest peak is the correlation intensity between Washington's image and Jefferson's image.

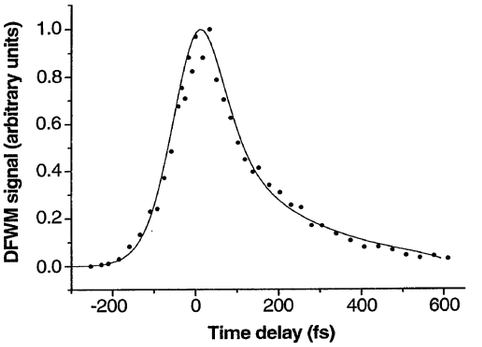

Fig. 3. Temporal profile of the degenerate four-wave mixing (DFWM) signal, when pumped with 90-fs pulses. The solid line is a fit to the DFWM signal as a function of pulse delay.

images of U.S. President George Washington; the next largest peak is the correlation intensity between Washington's image and President Thomas Jefferson's image. The two small peaks in the foreground are residual correlations between a rotated image of Washington and an image of President John Adams. Other residual peaks are noise; the signal-to-noise ratio is better than 10:1. The correlation intensity shows that Jefferson's image resembles Washington's image more closely than Adams' image. The correlation between Washington's image and the rotated image of Washington is greatly reduced, illustrating the rotational variance of four-wave mixing correlation.

The temporal profile of the degenerate four-wave mixing signal, when pumped with 90-fs pulses, is shown in Fig. 3. Measurement of the diffraction efficiency at zero time delay (η) yielded $\eta \approx 10^{-4}$. Because the pulsed laser operated at 620 nm, we were pumping into the leading edge of the π-π^* absorption band (*10*). Consequently, we expected the laser-induced gratings to have contributions from changes in the absorption coefficient ($\Delta\alpha$) and from changes in the index of refraction (Δn); the former leads to an amplitude grating and the latter to a phase grating. Changes in the index of refraction can arise from the third-order NLO properties [$\Delta n = n_2 I$, where I is the intensity of the pump beam and $n_2 \propto \mathrm{Re}\chi^{(3)}$] and from shifts in the oscillator strength resulting from the absorption. In this case, the diffraction efficiency is given by (*12*)

$$\eta = \frac{2\pi d^2}{4\lambda^2}\left[\Delta n^2 + \left(\frac{\Delta\alpha\lambda}{4\pi}\right)^2\right] \quad (1)$$

in the small η limit, where d is the thickness of the film and λ is the wavelength. One anticipates that any contribution to the gratings from n_2 will be instantaneous, whereas real excitations that lead to $\Delta\alpha$ (and the associated contribution to Δn) are expected to have a finite lifetime.

The full width at half maximum of the temporal profile is 160 fs (Fig. 3), with an asymmetry in the diffraction efficiency (η) associated with delaying the read beam. We have fit the temporal profile in Fig. 3 to the expression for the degenerate four-wave mixing signal as a function of the pulse delay, assuming that the signal comprised two components: an instantaneous component and a time-resolved component (*13*). The time-resolved component (with an amplitude of about 40% of the fast component) decayed exponentially with decay constant of about 450 fs. The exponential decay of the delayed response is consistent with that observed in photoinduced-absorption measurements (*14*), which yield a similar decay time for $(\Delta\alpha)^2$. Moving the pump frequency slightly farther into the infrared (so as to avoid pumping into the band edge) should avoid the creation of real excitations and thereby shorten the processor response time to about 115 fs (*13*). From Eq. 1, therefore, we conclude that the contribution from $\Delta n \propto n_2$ is the dominant term and that the actual image processing time of the material is less than 115 fs. The peak processing rates are, therefore, greater than 3×10^{16} operations per second. For comparison, Cray Research's fastest current supercomputer, the C916, attains a theoretical maximum processing rate of 1.55×10^{10} floating point operations per second. The average processing rate is limited by the nematic liquid-crystal SLMs; faster SLMs will be required before average processing rates can match the peak rate.

We tested the spatial resolution of the correlator by collimating the object and reference beams and modulating the read beam with a standard USAF-1951 resolution target. The resolution was better than 1.6 line pairs per millimeter over the 25-mm SLM aperture, equivalent to an array of 5000 pixels of information overall. This figure includes the resolution of the entire correlator including the SLMs and the NLO polymer sample.

REFERENCES AND NOTES

1. C. Halvorson, T. W. Hagler, D. Moses, Y. Cao, A. J. Heeger, *Chem. Phys. Lett.* **200**, 364 (1992).
2. F. Krausz, E. Wintner, G. Leising, *Phys. Rev. B* **39**, 3701 (1989).
3. V. Mizrahi, K. W. DeLong, G. I. Stegeman, M. A. Saifi, M. J. Andrejco, *Opt. Lett.* **14**, 1140 (1989).
4. C. Halvorson and A. J. Heeger, *Chem. Phys. Lett.* **216**, 488 (1993).
5. P. D. Foote *et al.*, *Appl. Opt.* **32**, 174 (1993).
6. Y. Owechko, G. J. Dunning, E. Marom, B. H. Sofer, *ibid.* **26**, 1900 (1987).
7. D. Psaltis, D. Brady, K. Wagner, *ibid.* **27**, 1752 (1988).
8. P. Yeh *et al.*, *Opt. Eng.* **28**, 328 (1989).
9. T. W. Hagler and A. J. Heeger, *Prog. Theor. Phys. Suppl.* **113**, 65 (1993); *Phys. Rev. B* **49**, 7313 (1994).
10. K. Pakbaz, R. Wu, F. Wudl, A. J. Heeger, *J. Chem. Phys.* **99**, 590 (1993).
11. C. Halvorson, R. Wu, D. Moses, F. Wudl, A. J. Heeger, *Chem. Phys. Lett.* **212**, 85 (1993).
12. H. J. Eichler, P. Günter, D. W. Pohl, *Laser-Induced Gratings* (Springer Series in Optical Sciences, vol. 50, Springer-Verlag, Berlin, 1986).
13. G. M. Carter, *J. Opt. Soc. Am. B* **4**, 1018 (1987).
14. B. Kraabel, in preparation.

15. Funding for the design and construction of the optical correlator and for the measurements presented in this report were provided by U.S. Air Force Office of Scientific Research grant AFOSR93-1-0191; the femtosecond laser was funded through an equipment grant by NSF. We thank K. Pakbaz for helpful discussions.

5 May 1994; accepted 13 July 1994